www.cafetinnova.org

ISSN 0974-5904, Volume 10, No. 02

DOI:10.21276/ijee.2017.10.0209

International Journal of Earth Sciences and Engineering

April 2017, P.P. 191-199

Vulnerability Assessment of Marine Structures: A Case Study on Jetty

CHENNA RAJARAM[1], RAMANCHARLA PRADEEP KUMAR[2], AJAY PRATAP SINGH[3], KAPIL MOHAN[3] AND BAL KRISHNA RASTOGI[3]

[1]*Earthquake Engineering Research Centre, IIIT-Hyderabad, Hyderabad, India*

[2]*Department of Civil Engineering, Earthquake Engineering Research Centre, IIIT-Hyderabad, Hyderabad, India*

[3]*Institute of Seismological Research, Gujarat, India*

Email: *rajaram.chenna@research.iiit.ac.in, ramancharla@iiit.ac.in*

Abstract: *Jetties are one of the most important structures in the coastal area, which can be used for transporting large quantities of goods and raw materials from one place to the other. Their functionality is very much essential because they are lifeline structures of the country. It is observed during the past earthquakes that jetties have been damaged even under mild shaking. Damaged and unserviceable jetties cause delay of export and import business. It directly affects the economy of particular region in terms of business, employment and growth. This clearly indicates the need to design these facilities so that they can withstand natural disasters particularly earthquakes and tsunamis. In this paper, a study has been carried out to find out the damage (D) to the Jetty. The Jetty is modeled using 2D Applied Element Method (AEM) to perform damage analysis of structure. Pushover analysis is done to get base shear vs roof displacement of building using displacement control method. Using the dissipated energy approach, damage is quantified at every displacement level and normalized to 1. A fragility curve has been developed to quantify the damage of Jetty with respect to different peak ground accelerations. The damage values were calculated for the PGA values of KHF Mandvi, NKF Jodiya and KMF Jhangi and found that the Jetty got light damage (D=0.2), and moderate damage (D=0.38 and 0.42) respectively.*

Keywords: *Jetty, non-linear analysis, fragility curve, damage*

1. Introduction

Jetties are one of the most important structures in coastal facilities which can be used for transporting large quantities of goods and raw materials from one place to another. Some of the coastal facilities at Kandla port site, and Navlakhi port sites were damaged during the 2001 Bhuj earthquake. The damaged and unserviceable port structures cause delay of export and import business. This directly affects the economy of the particular region in terms of business, employment & growth, which clearly indicates the need to design the coastal facilities which can withstand natural disasters particularly earthquakes and tsunamis.

A newly constructed Jetty at Navlakhi port, located on the Gulf of Kachchh, was severely damaged during the 2001 Bhuj earthquake. Flexural and shear cracks were observed at beam-column joint of the Jetty at Kandla port during the earthquake (Jain et al., 2001; Madabushi et al., 2005). The Jetty consists of an approach segment meeting the main berthing structure at an angle of 120^0. The pounding damage was observed at the intersection of approach and main berthing segment during the 2002 North Andaman earthquake as shown in figure 1 (Durgesh et al., 2002; Rajaram, 2011). The Jetty suffered moderate damage at Paracas during the recent 2007 Peru earthquake as shown in figure 2 (Fabio et al., 2009). Recent literature has been done on dynamic analysis and behavior of the Jetty.

A parametric study was done to analyze the forces on various members of the Jetty and the influence of different wave directions on these forces and moments. It is observed that the forces and moments are large as the diameter of pile increases and the deflection is reduced. From the time history analysis of the Jetty, it is observed that as the pile diameter increases the maximum deflection occurs at a larger time period (Shantala et al., 2011). A study has been done on dynamic analysis of the open piled Jetty of Sint Maarten in 2010 which was significantly damaged by hurricane. It is found that lower the natural frequencies of the Jetty, higher the wave frequencies (Bron et al., 2013). A large series of pushover analysis was performed on Jetty using PLAXIS 3D. Based on these analyses, it was concluded that P-Δ expressions yield good results (Besseling, 2012).

Received: December 22, 2016; Accepted: February 17, 2017; Published: April 26, 2017
International Journal of Earth Sciences and Engineering, 10(02), 191-199, 2017, DOI:10.21276/ijee.2017.10.0209

Figure 1. *Approach Jetty meets at an angle with the main berthing Jetty at Diglipur harbour. The damage to Jetty slab was concentrated at the intersection*

Figure 2. *Jetty structure damaged at Yacht Club in Paracas during 2007 Peru earthquake*

In this paper, a study has been conducted to study the damage of Jetty subjected to eight ground motions at Katrol Hill Fault (KHF) Bharuch, Dholera, Lalpur and Mandvi and Kachchh Mainland Fault (KMF) Bharuch, Dholera, Lalpur and Mandvi in the state of Gujarat. Later, the study has been continued on pushover analysis and further fragility analysis.

2. Modeling of Jetty

The Jetty is modeled in SAP2000V16.0 for preliminary analysis. Following are a few assumptions considered in the analysis:

- The analysis does not consider wind loads as the study mainly concentrates on seismic loads.
- Also, the structure has not been subjected to wave and current loads.

The geometry of the Jetty, material properties, boundary and loading conditions are given below.

2.1 Geometry details

A 450 m long and 45 m wide Jetty is considered in this analysis. The Jetty is supported by vertical piles arranged in a pattern that repeats for every 10 m. A concrete pile depth of 15 m with a circular cross section of 0.8 m is considered for the analysis. The thickness of deck slab is considered as 0.3 m. A 10 m and 6 m of spacing are considered between adjacent piles in longitudinal and transverse direction, respectively. A cross section of the Jetty along transverse direction is shown in figure 3. The geometry details of the Jetty are shown in table 1.

Table 1: *Geometry details of Jetty*

Structural Member	Dimensions
Total Jetty span Length	450 m
Total Jetty span width	45 m
Pier Diameter	0.8 m
Deck Slab Thickness	0.3 m
Distance Between Two piers in longitudinal Direction	10 m
Distance Between Two piers in Transverse Direction	6 m
Pile Depth	15 m

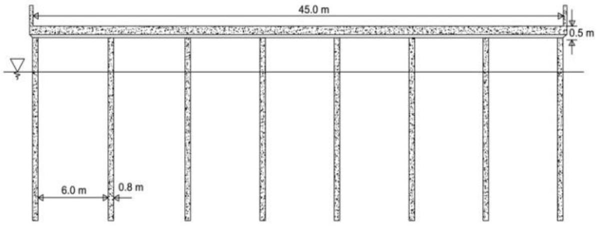

Figure 3. *Cross section details of Jetty used in the analysis*

2.2 Material properties

A M_{25} grade of concrete and a Poisson's ratio of 0.2 are used in the analysis. The same material properties are applied for the Jetty.

2.3 Boundary conditions

A fixed boundary condition is applied at the bottom of piles. The soil-structure-interaction has not been considered in the analysis.

2.4 Loading conditions

A dead load and live load of 8.1 kN/m^2 and 49 kN/m^2 are considered in the analysis (Jain S.K. et al., 2002). The total dead load and lateral load obtained from the analysis are 13.2 MN and 6.4 MN, respectively. A longitudinal reinforcement of twelve 28 mm diameter of bars and a lateral reinforcement of 10 mm diameter helical steel with spacing of 250 mm center to center are provided to the Jetty (Jain S.K. et al., 2002). The main objective of the study is to analyze the Jetty under seismic loading. For this purpose, the analysis has not been considered wave loads, wind loads, slapping loads and slamming loads. The effect of the Jetty due to above loads will be future scope of the study.

3. Numerical Modeling

The numerical techniques can be categorized in two ways. The first case assumes that the material as a continuum like Finite Element Method (FEM). The other category assumes that the material as a discrete model like Rigid Body Spring Model (RBSM), Extended Distinct Element Method (EDEM) and Applied Element Method (AEM) (Hatem, 1998).

The RBSM performs only in small deformation range. EDEM overcomes all the difficulties in FEM, but the accuracy is less than FEM in small deformation range. Till now, there is no method among all the available numerical techniques, by which the behavior of the structure from zero loading to total complete collapse can be calculated with high accuracy. Figure 4 represents the overview of numerical techniques. The overview of AEM is as follows:

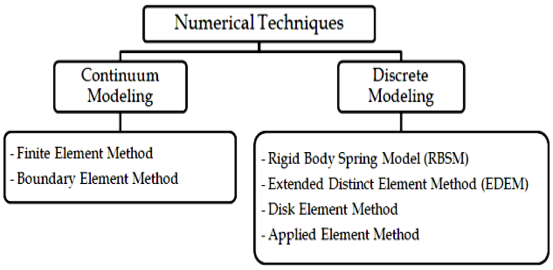

Figure 4. *Overview of numerical techniques*

3.1 Finite Element Method (FEM)

FEM is one of the most important techniques used in the analysis of structures. In this method, the elements are connected by nodes where the degrees of freedom are defined. The displacement, stresses and strains inside the element are related to the nodal displacements. The accuracy of the element depends on the size of the element. The analysis can be done on elastic and nonlinear materials with small and large deformations except for the ones with collapse behavior. At failure, the location of cracks should be defined before analysis, which is not possible in collapse analysis. The problem becomes much more complicated when the crack occurs in 3D problems. In this analysis, Takeda model is used (Pradeep et al., 2014). This model includes (a) stiffness changes at flexural cracking and yielding, (b) hysteresis points/rules for inner hysteresis loops inside the outer loop and (c) unloading stiffness degradation with deformation. The response point moves toward a peak of the one outer hysteresis loop. The problems in FEM are addressed in AEM and an overview of its methodology is described below.

3.2 Applied Element Method (AEM)

FEM could not simulate the complete collapse behavior of structures. Whereas, EDEM follows till the structural collapse of the structure, but its accuracy is less than FEM. The method which combines the advantages of both FEM and EDEM is AEM.

Applied element method is a discrete method in which the elements are connected by a pair of normal and shear springs which are distributed around the edges of the element. These springs represent the stresses and deformations of the studied element. The element's motion is a rigid body motion and the internal deformations are taken by springs only. The general stiffness matrix components corresponding to each degree of freedom are determined by assuming unit displacement and the forces are at the centroid of each element. The element stiffness matrix size is 6x6. The stiffness matrix component diagram is shown in figure 5 and the stiffness matrix is shown in figure 6. The global stiffness matrix is generated by summing up all the local stiffness matrices of each element.

The material model used in this analysis is Maekawa compression model (Hatem, 1998). In this model, the tangent modulus is calculated according to the strain at the spring location. After peak stresses, spring stiffness is assumed as a minimum value to avoid having a singular matrix. The difference between spring stress and stress corresponding to strain at the spring location is redistributed at each increment in reverse direction. When concrete springs are subjected to tension, spring stiffness is assumed as the initial stiffness till it reaches a crack point. After cracking, the stiffness of the springs subjected to tension is assumed to be zero. For reinforcement, bi-linear stress strain relationship is assumed. After the yield of reinforcement, the steel spring stiffness is assumed as 0.01 of initial stiffness. After reaching 10% of strain, it is assumed that the reinforcement bar be cut. The force carried out by the reinforcement bar is redistributed to the corresponding elements in the reverse direction. For cracking (Hatem, 1998), the failure criteria based on principal stresses is adopted. The models for concrete, both in compression and tension and the reinforcement bi-linear model are shown in figure 7.

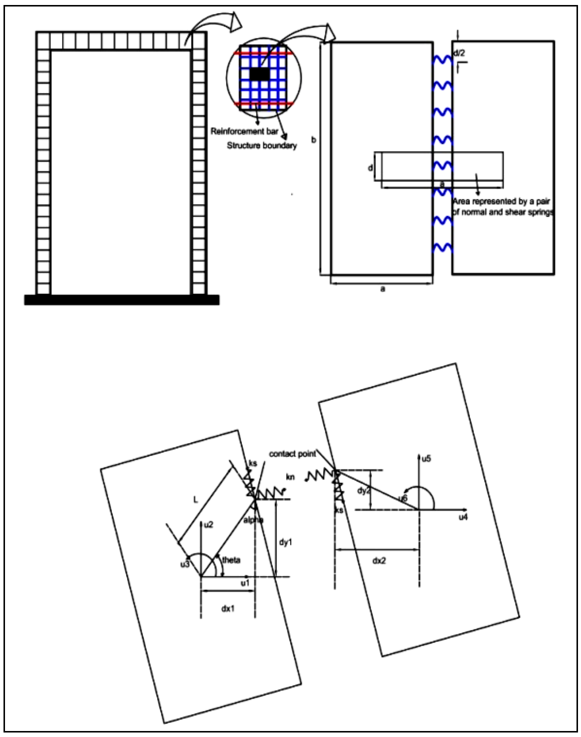

Figure 5. *Modeling of structure in AEM and element shape, contact point and dof*

$$\begin{bmatrix} S_{11} & S_{12} & S_{13} & -S_{11} & -S_{12} & S_{16} \\ S_{12} & S_{22} & S_{23} & -S_{21} & -S_{22} & S_{26} \\ S_{13} & S_{23} & S_{33} & -S_{31} & -S_{32} & S_{36} \\ S_{14} & S_{24} & S_{34} & S_{11} & S_{12} & S_{46} \\ S_{15} & S_{25} & S_{35} & S_{45} & S_{22} & S_{56} \\ S_{16} & S_{26} & S_{36} & S_{46} & S_{56} & S_{66} \end{bmatrix}$$

$$\begin{aligned} S_{11} &= k_n \sin^2(\theta+\alpha) + k_s \cos^2(\theta+\alpha) \\ S_{22} &= k_s \sin^2(\theta+\alpha) + k_n \cos^2(\theta+\alpha) \\ S_{33} &= k_n l^2 \cos^2(\alpha) + k_s l^2 \sin^2(\alpha) \\ S_{12} &= 0.5(\sin 2(\theta+\alpha))(k_s - k_n) \\ S_{13} &= k_s l \sin(\alpha)\cos(\theta+\alpha) - k_n l \cos(\alpha)\sin(\theta+\alpha) \\ S_{23} &= k_n l \cos(\alpha)\cos(\theta+\alpha) + k_s l \sin(\alpha)\sin(\theta+\alpha) \\ S_{16} &= -S_{11}dy + S_{12}dx - S_{13} \\ S_{26} &= -S_{12}dy + S_{22}dx - S_{23} \\ S_{36} &= -S_{13}dy + S_{23}dx - S_{33} \\ S_{46} &= S_{11}dy - S_{12}dx + S_{13} \\ S_{56} &= S_{12}dy - S_{22}dx + S_{23} \\ S_{66} &= -S_{16}dy + S_{26}dx - S_{36} \end{aligned}$$

***Figure 6.** Stiffness matrix at dof*

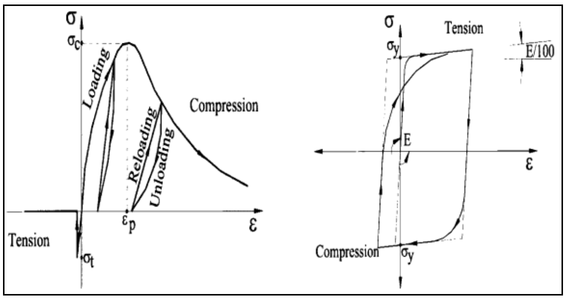

***Figure 7.** Material models for concrete and steel*

To determine the principal stresses at each spring location, the following technique is used in this analysis. The shear and normal stress components at point *A* are determined from the normal and shear springs attached at the contact point location as shown in the figure 8.

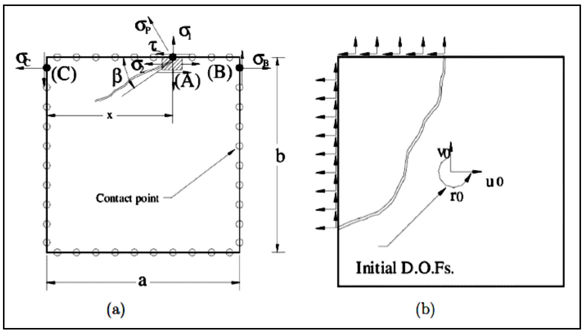

***Figure 8.** (a) Principal Stress determination and (b) Redistribution of spring forces at element*

The secondary stress σ_2 from the normal stresses at point *B* and *C* can be calculated by using the equation given below:

$$\sigma_2 = \frac{x}{a}\sigma_B + \frac{a-x}{a}\sigma_c \tag{1}$$

The principal tension is calculated as:

$$\sigma_P = \frac{\sigma_1 + \sigma_2}{2} + \sqrt{\left(\frac{\sigma_1 - \sigma_2}{2}\right)^2 + \tau^2} \tag{2}$$

The value of principal stress (σ_P) is compared with the tension resistance of the studied material. When σ_P exceeds the critical value of tension resistance, the normal and shear spring forces are redistributed in the next increment by applying the normal and shear spring forces in the reverse direction. These redistributed forces are transferred to the element center as a force and moment, and then these redistributed forces are applied to the structure in the next increment.

It is assumed that a failure inside the element is represented by the failure of attached springs (Hatem et al., 2000). If the spring fails, the force in the spring will redistributed. During this process, springs near the crack portion tend to fail easily. However, the main disadvantage of this technique is that the crack width cannot be calculated accurately. In each increment, stresses and strains are calculated for reinforcement and concrete springs. In case of springs are subjected to tension, the failure criterion is checked.

4. Nonlinear Time History Analysis of Jetty

A study has been conducted to understand the dynamic nonlinear behavior of Jetty. The dynamic properties of the Jetty are as follows: The fundamental periods in mode 1, mode 2, mode 3 and mode 4 are 1.27s, 1.24 s, 1.17 s and 1.07 s, respectively. The Jetty is subjected to eight ground motions, viz, KMF region (Bharuch, Dholera, Lalpur and Mandvi) and KHF (Bharuch, Dholera, Lalpur and Mandvi). These ground motions are obtained from the Institute of Seismological Research (ISR, Gujarat, India). The geographical locations of Dholera, Bharuch Lalpur and Mandvi are (Lat 22.25, Long 72.2), (Lat 21.74, Long 73.01), (Lat 22.35, Long 69.96) and (Lat 22.82, Long 69.35). The related ground motion records and its Fourier amplitude spectrums are shown in figure 9. The characteristics of each ground motion (amplitude, frequency content and strong ground motion duration) are calculated and listed in table 2 (Kramer, 2006). These characteristics play a major role in the non-linear time history response of Jetty.

***Table 2.** Details of characteristics of ground motions*

Region	Ground Motion	Amplitude (g)	Duration (s)	Frequency (Hz)
Katrol Hill Fault (KHF)	Bharuch	0.012	-	7.0-9.0
	Mandvi	0.308	21.50	6.3-8.5
	Lalpur	0.091	8.48	6.2-9.5
	Dholera	0.013	-	5.8-7.1
Kachchh Mainland Fault (KMF)	Bharuch	0.018	-	6.7-9.2
	Mandvi	0.122	14.80	5.5-8.5
	Lalpur	0.086	11.00	6.2-9.6
	Dholera	0.021	-	5.8-7.1

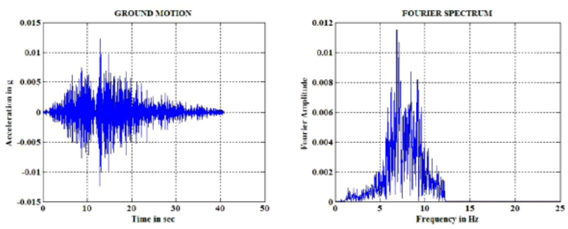

KHF Bharuch

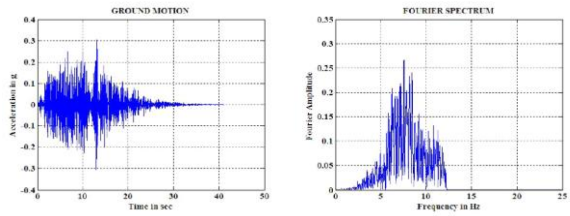

KHF Mandvi

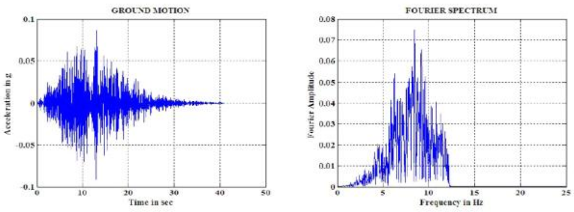

KHF Lalpur

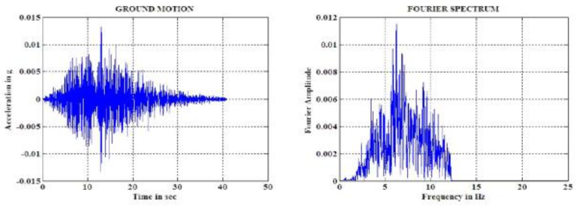

KHF Dholera

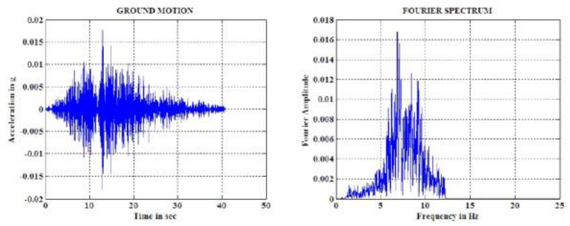

KMF Bharuch

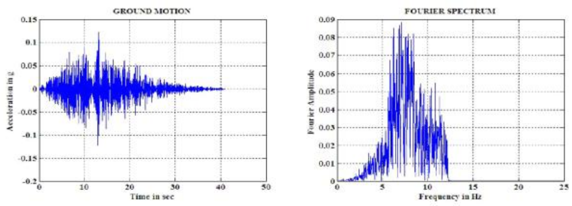

KMF Mandvi

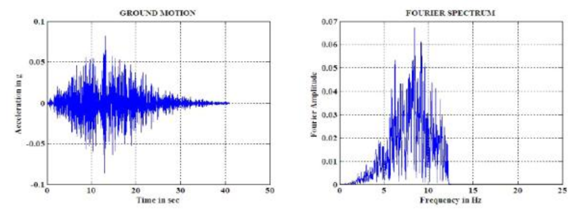

KMF Lalpur

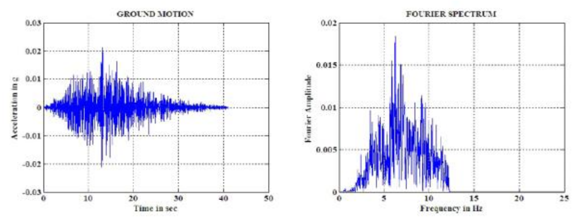

KMF Dholera

***Figure 9**. Ground motion records and corresponding Fourier amplitude spectra*

The displacement response of the Jetty is calculated using Newmark's beta method (Chopra, 2006). In numerical study, it is important to fix the element size. As the element size decreases, the results tend to converge. For this purpose, the response is initially calculated with an element size of 0.25 m. As the size of element decreases, the response level gets saturated. This means the response will be same with further decrease in the element size. Based on the element size of 0.25 m, the Jetty is modeled both in 2D and 3D (Ref: figure 10). The nonlinear responses are plotted in figure 11. For all the ground motions, the response is calculated at the top of Jetty. From table 2, the predominant frequency range of ground motions is 0.11-0.18 s which is far from the fundamental period of the Jetty. The responses are calculated along the flexible direction of the Jetty. The displacement responses of the Jetty are 2.0E-6, 2.0E-6, 1.42E-5, 4.52E-5, 3.54E-5, 3.09E-6, 1.3E-5 and 1.8E-5 m. From the analysis, the maximum response obtained from KHF Mandvi ground motion is 4.52E-5 m. This is because of high PGA value among all the ground motions. But, the response of the Jetty will effect because of frequency, not from the PGA. It would experience more response if the fundamental period falls in the range of predominant frequency/period of ground motion (Pradeep et al., 2014). But, in this case, the fundamental period of the Jetty is too far from the predominant frequency/period of the ground motion. The frequency range of ground motions is 5-10 Hz and the fundamental frequency of the structure is 0.78 Hz, which is far from the frequency range of ground motions. From the analysis, it is observed that the nonlinear response of the structure is similar to that of the linear analysis. It means that the structure has not yielded for the ground motions it is subjected to.

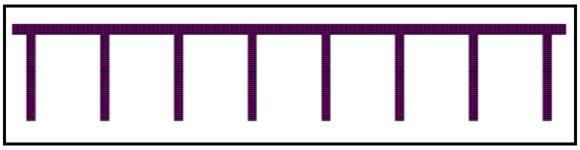

AEM 2D modeling of Jetty

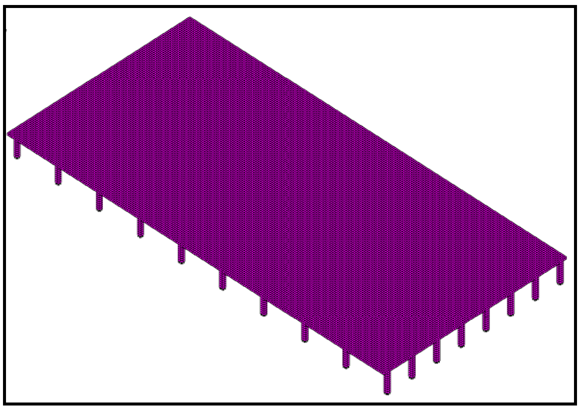

AEM 3D modeling of Jetty

***Figure 10.** Modeling of Jetty in AEM*

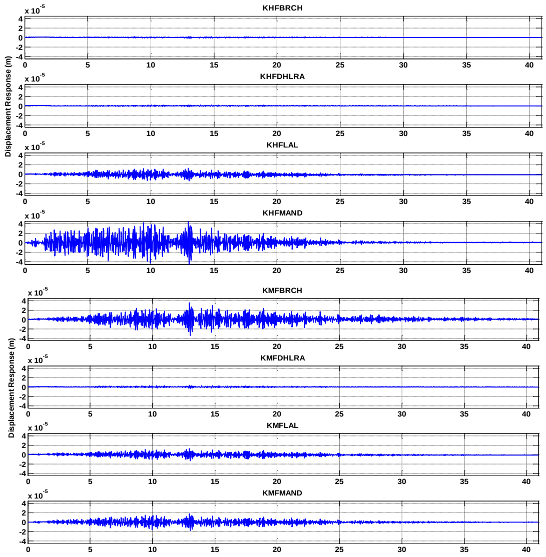

Figure 11. *Displacement response of the Jetty at different locations in Gujarat*

4.1 Response due to amplified ground motions

Gujarat state is under seismic zone III, IV and V. The ground motions are generated at places along the coastline of Gujarat. The upper coastal line of Saurashtra region is under seismic zone IV and coastal line of Kachchh region is under seismic zone V. As per IS: 1893-2007, the seismic zone factor for IV and V are 0.24 g and 0.36 g respectively. To understand the behavior of the Jetty under these seismic zones, the ground motions are normalized to 0.24 g and 0.36 g. The normalized ground motions are applied to the Jetty.

A comparison is done for the responses of the Jetty due to amplified ground motions. The 2D responses reasonably match with the 3D responses. From both the analyses, there is a slight increase in the responses due to amplified ground motions for 0.24 g and 0.36 g. It is because of variation of the time period of structure from both the analyses. The summary of the responses due to amplified ground motions is listed in table 3. The displacement responses are shown in figure 12 and 13.

Table 3. *Maximum displacement responses for ground motions normalized to 0.24 and 0.36 g (AEM)*

Region	Ground Motion	Max. Displacement Response (m) – 0.24g	Max. Displacement Response (m) – 0.36g
Katrol Hill Fault (KHF)	Bharuch	2.2×10^{-4}	3.4×10^{-4}
	Dholera	3.1×10^{-4}	4.7×10^{-4}
	Lalpur	1.5×10^{-4}	2.3×10^{-4}
	Mandvi	1.7×10^{-4}	2.6×10^{-4}
Kachchh Mainland ult (KMF)	Bharuch	2.0×10^{-4}	3.4×10^{-4}
	Dholera	3.0×10^{-4}	4.6×10^{-4}
	Lalpur	1.4×10^{-4}	2.1×10^{-4}
	Mandvi	1.6×10^{-4}	2.4×10^{-4}

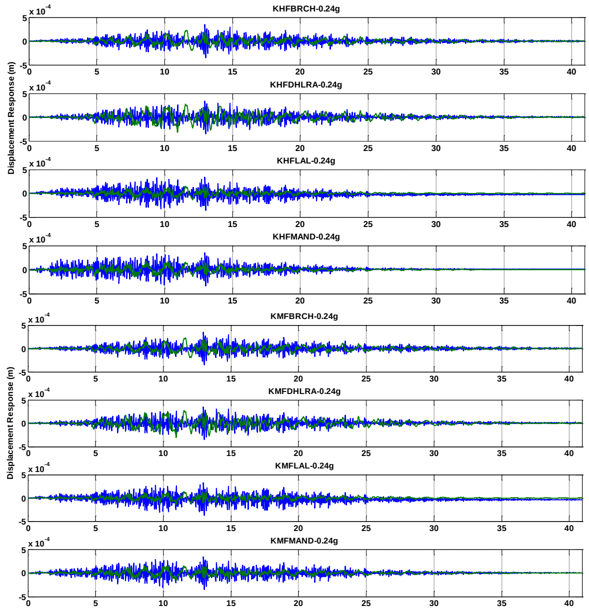

Figure 12. *Comparison of AEM & FEM responses for ground motions normalized to 0.24g*

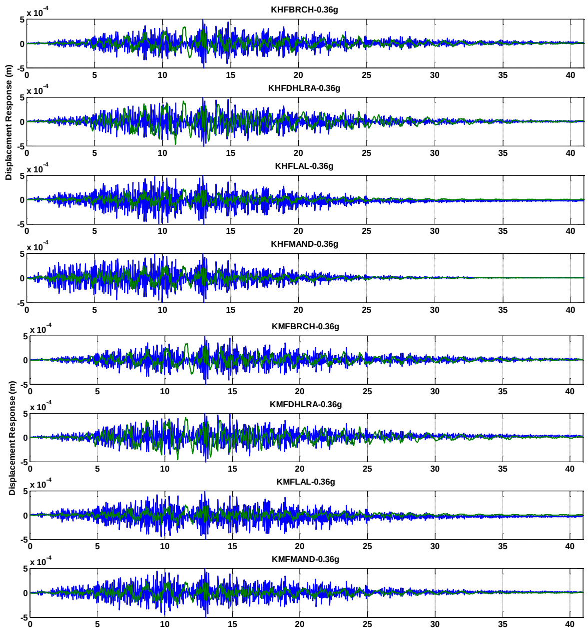

Figure 13. *Comparison of AEM & FEM responses for ground motions normalized to 0.36g*

5. Pushover Analysis

Pushover analysis is mainly to evaluate existing buildings and retrofit them. It can also be applied for new structures. Structures would become massive and uneconomical if they were to be designed to behave elastically during earthquakes. Therefore, the structures must undergo some damage to dissipate seismic energy. To design such a structure, it is necessary to know its performance and collapse pattern (Amin et al., 2010). To know performance and collapse pattern, a static non-linear procedure is helpful. Nonlinear static procedures are incremental static analyses used to determine the force-displacement relationship, or the capacity curve, for a structure. The analysis involves applying horizontal loads, in a prescribed pattern, onto the structure, incrementally pushing the structure and plotting the total applied lateral force and associated lateral displacement at each increment, until the structure achieves collapse condition. A plot of the total base shear versus roof displacement in a structure is obtained by this analysis that would indicate any premature failure or weakness.

The structure is pushed using either load control or displacement control to obtain the load versus displacement curve of a structure. In this analysis, the displacement control is used till 60% of maximum strength after attaining peak strength. The effect of plastic hinges is incorporated in this analysis. The failure locations, cracking in concrete and yield of steel are determined automatically.

The stiffness of the structure starts getting reduced when the first crack takes place or when the first spring fails. The first yield takes place in the second column at X coordinate 6.5 m and Y coordinate 16.6 m. In this analysis, the steel failure is also allowed. The load initially increases with increase of displacement till structure attains maximum load. Later, the load decreases with further increase of displacement (Ref: figure 14). The analysis is further carried out to calculate damage of the Jetty subjected to the PGA values of KHF Mandvi, NKF Jodiya and KMF Jhangi. The fragility analysis will be discussed in the following section.

6. Fragility Analysis

A new method is proposed based on energy to estimate the damage of the structure. The total dissipated energy of the structure is obtained from the area under the pushover curve. The damage index (D_i) is expressed as the ratio of inelastic energy to the total inelastic energy capacity of the structure. The initial elastic energy (E_{ie}) is calculated as the area under the curve up to a point which is the first yield point of the structure. E is the energy absorbed by the structure, up to any point in the pushover curve, where the damage is to be calculated.

The total nonlinear energy capacity (ET) of the structure is calculated as the total area under the pushover curve (Pradeep et al., 2014). The elastic and inelastic energies of the structure are calculated at each displacement in the pushover curve. The schematic diagram represents a calculation of damage from pushover curve shown in figure 15 (Pradeep et al., 2014). The damage parameter (D) is denoted as the ratio of inelastic energy to the total energy of the structure. Damage parameter is a dimensionless quantity. The dissipated energy at point *'i'* is inelastic energy in damage calculation. The dissipated energy till collapse gives rise to the total energy in damage calculation.

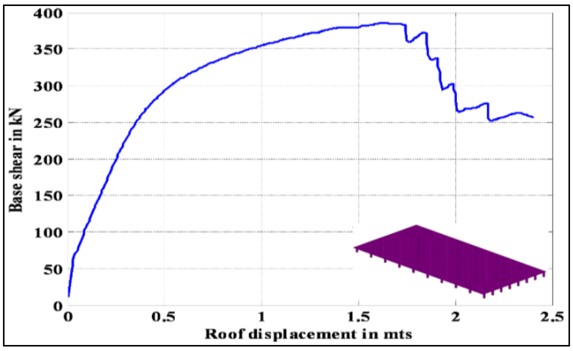

Figure 14. *Base shear vs roof displacement for Jetty*

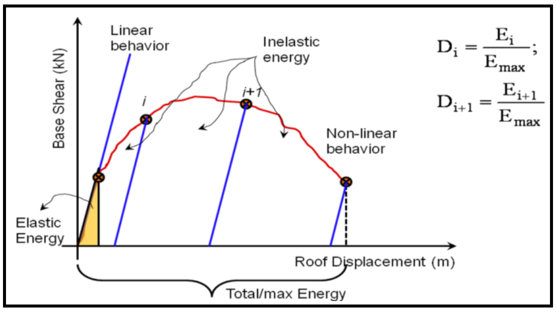

Figure 15. *Schematic diagram represents Base shear vs Roof displacement of Jetty to calculate damage*

Following is the procedure to convert from spectral displacements to accelerations of structure.

Step-1: The spectral accelerations (*Sa*) are calculated using $4\pi(SD)/T^2$. Where SD=spectral displacement and T=time period.

Step-2: The spectral displacement (*SD*) values are calculated from base shear relation

$$V = \alpha . S_a W;$$
$$\Delta_{roof} = PF.SD.\phi_{roof};$$
$$SD = \frac{\Delta_{roof}}{PF.\phi_{roof}} \tag{3}$$

Where, V-base shear, W-seismic weight of structure, PF-participation factor.

A fragility curve has been drawn with the obtained damage values with respect to acceleration. Figure 16 represents spectral accelerations from response spectra of KHF Mandvi, NKF Jodiya and KMF Jhangi. Figure 17 shows the damage curve of Jetty for different PGA values of ground motion.

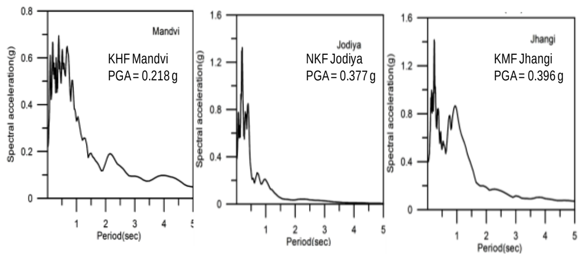

Figure 16. *Spectral accelerations from response spectra of KHF Mandvi, NKF Jodiya and KMF Jhangi (Source: ISR, Gujarat)*

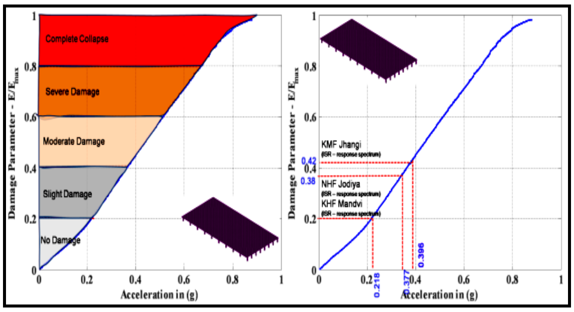

***Figure 17**. Fragility curve of Jetty subjected to KHF Mandvi, KMF Jhangi and NHF Jodiya*

The following fragility curve is developed from the PGA values given by ISR. The PGA values at KHF Mandvi, NKF Jodiya and KMF Jhangi stations are 0.218g, 0.377 g and 0.396g respectively. From the analysis, it is clear that the damage of the Jetty is 0.2, 0.38 and 0.42 for KHF Mandvi, NHF Jodiya, and KMF Jhangi respectively. The damage of Jetty is calculated 0.2 (Light damage), 0.38 (Moderate damage) and 0.42 (Moderate damage) respectively.

7. Conclusions

In this paper, a study has been carried out to find out the damage of the Jetty. The Jetty has analyzed and modeled using 2D AEM to perform damage of the structure. A nonlinear time history analysis was conducted to understand the behavior of the Jetty subjected to eight ground motions. It was found that the response of the Jetty was similar to the linear time history analysis, as the predominant frequency range of ground motions is far from the fundamental natural period of the structure. It means that the structure is affected due to frequency, not because of amplitude of ground motion.

A damage model was proposed based on the dissipated energy from pushover curve. The damage states of the structure were defined as no damage (D<0.2), slight damage (D<0.4), moderate damage (D<0.6), severe damage (D<0.8) and complete collapse (D>0.8). The damage values were calculated for the PGA values of KHF Mandvi, NKF Jodiya and KMF Jhangi and found that the Jetty got light damage (D=0.2), and moderate damage (D=0.38 and 0.42) respectively.

Acknowledgements

This research was financially supported by the Ministry of Earth Science, Government of India and is hereby gratefully acknowledged.

References

[1] Amin K (2010) *Performance Based Seismic Vulnerability Evaluation of Existing Buildings in Old Sectors of Quebec*, Ph.D Thesis, University of Quebec.

[2] Besseling F (2012) *Soil-Structure Interaction Modeling in Performance Based Seismic Jetty Design*, Master of Science Thesis, Department of Civil Engg., Delft University of Technology, Netherlands.

[3] Bron VAG (2013) *Dynamic Analysis of an Open Piled Jetty Subjected to Wave Loading*, Master of Science Thesis, Department of Civil Engg., Delft University of Technology, Netherlands.

[4] Chopra AK (1995) *Dynamics of Structures - Theory and Applications to Earthquake Engineering*, Prentice Hall International Series.

[5] Durgesh CR and Murty CVR (2002) *Reconnaissance Report on North Andaman Earthquake of 14 September 2002*, Department of Civil Engineering, Indian Institute of Technology, Kanpur, India.

[6] Fabio T, John EA and Emily S (2007) August 15 Magnitude 7.9 Earthquake Near the Coast of Central Peru: Analysis and Field Mission Report. *Bulletin of Earthquake Engineering*. **7**: 1-70.

[7] Jain SK, Murty CVR, Umesh D, Jaswanth NA and Sailender KC (2001) *A Field Report on Structural and Geotechnical Damages Sustained During the 26 January 2001 M7.9 Bhuj Earthquake in Western India*, Department of Civil Engineering, Indian Institute of Technology, Kanpur, India.

[8] Kramer SL (2006) *Geotechnical Earthquake Engineering*, Pearson Education.

[9] Madabushi SPG and Haigh SK (2005) *The Bhuj, India Earthquake of 26 January 2001*, A Field Report by EEFIT, Institution of Structural Engineers, London.

[10] Pradeep KR and Murty CVR (2013) Critical Review of Indian Seismic Code; IS:1893-2002 *Proc. of International Colloquium on Architecture & Structural Interaction for Sustainable Development*, New Delhi, India.

[11] Pradeep KR, Srikanth T, Rajaram C, Rastogi BK, Santosh KS, Ajay C and Kapil M (2014) *Vulnerability Assessment of Port Buildings*. Technical Report No: IIIT/TR/2014/23, Earthquake Engineering Research Centre, International Institute of Information Technology, Hyderabad, India.

[12] Rajaram C (2011) *A Study of Pounding Between Adjacent Buildings*, Master of Science Thesis, Computer Aided Structural Engineering, International Institute of Information Technology, Hyderabad, India.

[13] Santala B, Subbarao, Venkataramana K and Harish (2011) Analysis of Berthing Structures for Wave Induced Forces. *International Journal of Earth Sciences and Engineering.* **4:** 112-121.

[14] Tagel DH (1998) *A New Efficient Method for Nonlinear, Large Deformation and Collapse Analysis of Structures*, Ph.D Thesis, Department of Civil Engineering, University of Tokyo, Tokyo.

[15] Tagel DH and Meguro K (2000) Applied Element Method for Simulation of Nonlinear Materials: Theory and Application for RC Structures.

Structural Engineering/Earthquake Engineering, *JSCE* **17**: 137–148.
[16] BIS (2007) IS:1893-2007 (draft). Criteria for earthquake resistant design of structures, part-1 general provisions and buildings, Bureau of Indian standards, New Delhi, India.